Mineralogical Magazine, August 2006, Vol. 70(4), pp. 347–359

Compositional evolution and cryptic variation in pyroxenes of the peralkaline Lovozero intrusion, Kola Peninsula, Russia

L. N. KOGARKO[1], C. T. WILLIAMS[2,*] AND A. R. WOOLLEY[2]

[1] Vernadsky Institute, Kosygin Street 19, Moscow 117975, Russia
[2] Department of Mineralogy, Natural History Museum, Cromwell Road, London SW7 5BD, UK

ABSTRACT

The Lovozero alkaline massif is the largest of the world's layered peralkaline intrusions (~650 km^2). We describe the evolution of clinopyroxene from the liquidus to the late residual stage throughout the whole vertical section (2.5 km thick) of the Lovozero Complex. Microprobe data (~990 analyses) of the clinopyroxenes define a relatively continuous trend from diopside containing 15–20% hedenbergite and 10–12% aegirine components, to pure aegirine. The main substitutions during the evolution of the Lovozero pyroxenes are (Na,Fe^{3+},Ti) for (Ca,Mg,Fe^{2+}). The composition of the pyroxene changes systematically upwards through the intrusion with an increase in Na, Fe^{3+} and Ti and decrease in Ca and Mg.

The compositional evolution of the Lovozero pyroxene reflects primary fractionation processes in the alkaline magma that differentiated *in situ* from the bottom to the top of the magma chamber as a result of magmatic convection, coupled with the sedimentation of minerals with different settling velocities.

The temperature interval of pyroxene crystallization is very wide and probably extends from 970 to 450ºC. The redox conditions of pyroxene crystallization in the Lovozero intrusion were relatively low, approximating the QFM buffer.

KEYWORDS: Lovozero, evolution of alkaline clinopyroxenes, cryptic layering, peralkaline magma.

Introduction

THE entire evolution of pyroxene-bearing magmatic systems, from the liquidus to the late residual stage, including subsolidus reactions, is often recorded in the compositions of the clinopyroxenes. This has been particularly well demonstrated for the alkaline rocks in which significant differences in pyroxene evolution are controlled by such factors as magma composition, alkalinity and oxygen fugacity (Larsen, 1976; Jones, 1984).

The Lovozero alkaline complex, the largest of the world's layered peralkaline intrusions, covers 650 km^2 and is situated in the central part of the Kola Peninsula, north-western Russia (Bussen and Sakharov, 1972; Kogarko *et al*., 1995). It is emplaced in Archaean granite gneisses and comprises a lopolith-like massif with a broad feeding channel located in the southwestern part of the intrusion (Kogarko *et al*., 1995; Arzamastsev *et al*., 1998). The complex was formed in four distinct intrusive phases. The oldest rocks (Phase 1) are poikilitic, even-grained feldspathoidal syenites that are located in the lowermost part of the intrusion and also found as xenoliths throughout the massif. These rocks are mostly miaskitic, i.e. with a coefficient of agpaicity <1 (coefficient of agpaicity is equal to the mole ratio $((Na_2O+K_2O)/Al_2O_3)$. The main rock-forming minerals are K-Na feldspar, nepheline, nosean, aegirine-diopside and magnesio-riebeckite with typical accessory minerals including ilmenite, magnetite, titanite, apatite and mosandrite.

The second phase (Phase 2), also known as the Differentiated Complex, consists of layered units ranging in thickness from a few centimetres to hundreds of metres, which from bottom to top

* E-mail: T.Williams@nhm.ac.uk
DOI: 10.1180/0026461067040340

comprise urtite, foyaite and lujavrite rock types. These three rock types of each unit grade into each other through intermediate varieties with sharp contacts only occurring between the urtite and underlying lujavrite. The total thickness of the Differentiated Complex is 2400 m. The rocks of Phase 2 are more alkaline than those of Phase 1 with a coefficient of agpaicity >1, and they contain abundant peralkaline minerals. Here, the rock-forming minerals are nepheline, microcline, sodalite, aegirine and arfvedsonite with the main accessory phases eudialyte, lamprophyllite, lomonosovite-murmanite, apatite, loparite, villiaumite, titanite, sodalite and lorenzenite (Table 1).

Phase 3, also known as the Eudialyte Complex, forms a plate-like body up to 450 m thick cutting the upper part of the Differentiated Complex. The plane of contact between rocks of Phases 2 and 3 dips towards the centre of the complex with the angle increasing from the margins towards the centre. The rocks of Phase 3 are more coarsely layered than those of Phase 2, and include leuco-, meso- and melanocratic eudialyte lujavrites. Veins of porphyritic lujavrite, which are late derivates of Phase 3, cut the rocks of Phases 1 and 2. The principal rock-forming minerals of Phase 3 are nepheline, microcline, aegirine, eudialyte, lamprophyllite and arfvedsonite. Eudialyte in this complex is euhedral, which is the principal difference from that in the lujavrite of Phase 2, where it is interstitial. The common accessory minerals are lomonosovite-murmanite, loparite, lovozerite, pyrochlore, lamprophyllite and sodalite. In some parts of the intrusion it is possible to see the reaction between alkaline magma of Phase 3 with the country rocks of the roof, resulting in the formation of titanite, apatite and amphibole-rich rocks (Gerasimovsky *et al*., 1966).

The rocks of Phase 4 comprise rare dykes of alkaline lamprophyres (monchiquite, fourchite, tinguaite, etc.) that cut all the earlier alkaline rocks as well as the surrounding granite gneisses.

The first data on the pyroxenes of Lovozero were presented by Vlasov *et al*. (1966) and Gerasimovsky *et al*. (1966). These, and more recent work by Korobeynikov and Laaioki (1994), established that the pyroxenes are enriched in the aegirine component. However, the compositional evolution of the pyroxenes through the layered sequence of the intrusion has not been investigated in detail.

The specimens studied in this paper were collected mostly from seven drill holes (numbers 469, 904, 521, 178, 144, 207 and 905) that sampled a complete stratigraphic section through the Lovozero massif of ~2400 m, with the exception of the middle zone of the Differentiated Complex, for which specimens were obtained from surface outcrop. A total of 988 microprobe analyses of pyroxene were obtained from 125 samples. Thus, we were able to investigate, for the first time, the evolution of the pyroxenes through the complete, accessible layered series of Lovozero.

Petrography

Comprehensive petrographic descriptions of Lovozero rocks are given by Vlasov *et al*. (1966), Gerasimovsky *et al*. (1966), and Bussen and Sakharov (1972), so only brief petrographic notes with emphasis on the pyroxenes will be given here.

TABLE 1. Mineral formulae for the 'exotic' mineral phases of Lovozero.

Mineral name	Formula
Eudialyte	$Na_{15}Ca_6(Fe^{2+},Mn^{2+})_3Zr_3(Si,Nb)(Si_{25}O_{73})(O,OH,H_2O)_3(Cl,OH)_2$
Lamprophyllite	$Na_2(Sr,Ba)_2Ti_3(SiO_4)_4(OH,F)_2$
Lomonosovite	$Na_2Ti_2\ Si_2O_9.Na_3\ PO_4$
Loparite-(Ce)	$(Ce,Na,Ca)(Ti,Nb)O_3$
Lorenzenite	$Na_2Ti_2Si_2O_9$
Lovozerite	$Na_2Ca(Ti,Zr)Si(O,OH)_{18}$
Mosandrite*	$(Ca,Na,Ce)_{12}(Ti,Zr)_2Si_7O_{31}H_6F_4$
Murmanite	$Na_2(Ti,Nb)_2Si_2O_9.nH_2O$
Villiaumite	NaF

* from Clark (1993); all others from Mandarino (1999)

The pyroxene in rocks of Phase 1 is cumulus and forms euhedral, elongate prisms and sometimes aggregates, but most commonly it forms masses of tiny prisms in interstitial patches between feldspar and nepheline, as well as large interstitial grains. It is zoned from light greenish-brown cores to deep-green rims; pleochroism is usually weak. The paler-coloured pyroxene is replaced by later aegirine and amphibole along cleavages and in the marginal parts of grains.

In the urtite and foyaite of the Differentiated Complex the pyroxene, which is both a cumulus and intercumulus mineral, commonly forms both large and small prismatic crystals, the former always poikilitically enclosing nepheline. In many examples, aggregates of skeletal and fibrous pyroxene occur in the spaces between nepheline and K feldspar. In lujavrite, the pyroxene is generally a cumulus phase and forms acicular and stout prismatic grains, sometimes orientated to give a trachytic texture. The pyroxene is intimately associated and intergrown with arfvedsonite and accessory minerals. In the Differentiated Complex, pyroxene crystals are strongly zoned, with pale yellow to colourless cores, and rims an intense green colour. In backscattered electron images, the cores often have a relatively higher mean atomic number than the rims (Fig. 1) because of much higher Ca/Na ratios in cores as compared with the rims. In some examples this zonation is reversed and patchy zoning occurs, which is usually characteristic of very late reactions with residual melts or a fluid phase.

The Eudialyte Complex contains the highest concentration of pyroxene, and it increases in abundance in the upper part of the complex. In the Eudialyte Complex the pyroxene is cumulus and usually present in the form of 'streams' of prismatic and acicular crystals. This is especially the case in the porphyritic lujavrites in which pyroxene forms phenocrysts, which are aligned together with masses of acicular, orientated crystals (Fig. 2).

Aegirine also occurs as tiny (1–2 μm) inclusions in nepheline in all the intrusive phases at Lovozero. We observed a correlation between the Fe content of nepheline and the presence or absence of included aegirines. Nepheline containing up to 2.3% FeO does not have aegirine inclusions, whereas in nepheline-containing aegirine, the Fe concentration drops to 0.1% or less. We believe that Fe-rich nepheline is a surviving solid solution and that aegirine inclusions in nepheline represent exsolution from the nepheline.

In all the Lovozero rocks, the nepheline and K-feldspar crystallized prior to clinopyroxene and amphibole, owing to the agpaitic order of crystallization, which is typical for peralkaline nepheline syenites.

Compositional evolution of the pyroxenes

Analyses were undertaken using a Cameca SX50 wavelength-dispersive electron microprobe and a Hitachi S2500 scanning electron microscope with an Oxford Instruments AN10000 energy-dispersive system at the Natural History Museum, London. Representative analyses of Lovozero pyroxenes are given in Table 2 and illustrated in Figs 3, 4 and 5, with all Fe given as Fe_2O_3, and

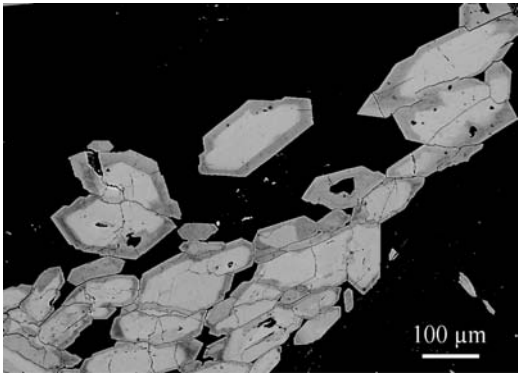

FIG. 1. BSE image illustrating the zoning in pyroxenes in the Differentiated Complex (sample Lovo 9).

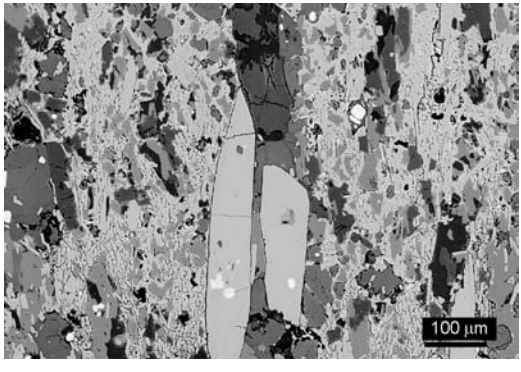

FIG. 2. BSE image showing two generations of pyroxene in porphyritic lujavrites from the Eudialyte Complex. In the centre are two clinopyroxene phenocrysts aligned with smaller, acicular, second-generation clinopyroxene.

TABLE 2. Representative microprobe analyses (wt.%) of pyroxene.

Depth (m)	Sample no	SiO_2	TiO_2	Al_2O_3	Fe_2O_3	MnO	MgO	CaO	Na_2O	NiO	Cr_2O_3	ZrO_2	Total
370	178-30	51.9	2.84	0.75	27.0	0.50	1.60	3.63	11.7	n.d.	b.d.l.	b.d.l.	99.9
224	144-163	52.2	3.68	0.94	26.2	0.53	1.65	2.75	11.8	0.11	b.d.l.	b.d.l.	100.0
126	133-225	52.5	2.13	0.97	27.1	0.45	2.00	4.17	11.3	0.05	b.d.l.	0.84	101.5
−133	521-398	52.5	1.86	0.80	26.0	0.63	2.58	5.64	10.5	0.06	0.08	b.d.l.	100.7
−350	97/2	51.1	1.83	0.85	25.7	0.59	2.71	6.18	10.1	b.d.l.	0.28	1.35	100.7
−500	VI	51.2	2.10	1.19	24.9	0.46	2.62	5.62	10.3	b.d.l.	0.49	1.31	100.1
−677	469-96	52.3	1.91	0.84	25.0	0.70	2.94	6.73	9.78	b.d.l.	0.05	b.d.l.	100.2
−900	Lovo 13	51.0	1.81	0.87	24.9	0.51	2.90	6.13	10.9	b.d.l.	b.d.l.	0.86	99.9
−1138.3	Lovo 116	51.1	1.60	0.99	24.4	0.50	3.14	6.56	9.85	b.d.l.	b.d.l.	1.09	99.2
−1275	469-679	51.9	1.60	0.85	24.0	0.57	3.76	8.25	8.97	0.38	0.19	b.d.l.	100.4
−1449	904-889	51.6	1.46	0.87	24.1	0.50	3.78	8.77	8.57	0.04	b.d.l.	b.d.l.	99.7
−1519	904-969	51.0	1.72	1.03	23.2	0.69	3.72	8.13	8.59	0.08	b.d.l.	b.d.l.	98.1
−1733	904-1183	51.9	1.40	1.09	23.8	0.61	3.99	9.50	8.36	b.d.l.	b.d.l.	b.d.l.	100.7
−1883	904-1333	51.6	1.60	1.49	23.8	0.57	3.24	7.08	9.34	0.12	0.20	b.d.l.	99.0
Phase	1 14	52.8	1.17	0.62	26.2	0.68	2.84	6.05	10.4	b.d.l.	b.d.l.	1.03	101.8
Phase	1 16	51.5	1.26	0.35	17.6	0.60	7.25	14.1	5.10	b.d.l.	b.d.l.	0.86	98.6
		cations to 6 oxygens											
		Si	Ti	Al	Fe^{3+}	Mn	Mg	Ca	Na	Ni	Cr	Zr	Sum
370	178-30	1.97	0.08	0.03	0.77	0.02	0.09	0.15	0.86	0.00	0.00	0.00	3.98
224	144-163	1.97	0.10	0.04	0.75	0.02	0.09	0.11	0.87	0.00	0.00	0.00	3.96
126	133-225	1.97	0.06	0.04	0.76	0.01	0.11	0.17	0.82	0.00	0.00	0.02	3.96
−133	521-398	1.98	0.05	0.04	0.74	0.02	0.14	0.23	0.76	0.00	0.00	0.00	3.96
−350	97/2	1.94	0.05	0.04	0.73	0.02	0.15	0.25	0.74	0.00	0.01	0.02	3.96
−500	VI	1.95	0.06	0.05	0.71	0.01	0.15	0.23	0.76	0.00	0.01	0.02	3.96
−677	469-96	1.98	0.05	0.04	0.71	0.02	0.17	0.27	0.72	0.00	0.00	0.00	3.95
−900	Lovo 13	1.95	0.05	0.04	0.72	0.02	0.17	0.25	0.80	0.00	0.00	0.02	4.01
−1138.3	Lovo 116	1.96	0.05	0.04	0.70	0.02	0.18	0.27	0.73	0.00	0.00	0.02	3.97
−1275	469-679	1.96	0.05	0.04	0.68	0.02	0.21	0.33	0.66	0.01	0.01	0.00	3.96
−1449	904-889	1.96	0.04	0.04	0.69	0.02	0.21	0.36	0.63	0.00	0.00	0.00	3.95
−1519	904-969	1.96	0.05	0.05	0.67	0.02	0.21	0.34	0.64	0.00	0.00	0.00	3.95
−1733	904-1183	1.95	0.04	0.05	0.67	0.02	0.22	0.38	0.61	0.00	0.00	0.00	3.95
−1883	904-1333	1.97	0.05	0.07	0.68	0.02	0.18	0.29	0.69	0.00	0.01	0.00	3.95
Phase	1 14	1.98	0.03	0.03	0.74	0.02	0.16	0.24	0.75	0.00	0.00	0.02	3.97
Phase	1 16	1.96	0.04	0.02	0.51	0.02	0.41	0.58	0.38	0.00	0.00	0.02	3.92

All Fe as Fe_2O_3; b.d.l. = below detection limit; n.d. = not determined. For details of depth, see text and Fig. 5

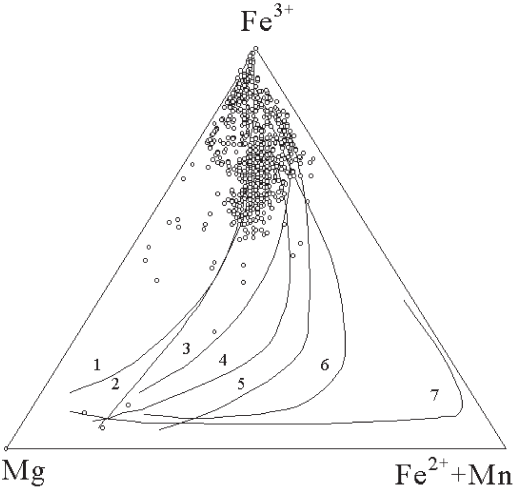

FIG. 3. Lovozero pyroxenes plotted in the (Mg), (Fe^{3+}), (Fe^{2+} + Mn) ternary diagram. For comparison, pyroxene trends from selected alkaline occurrences are illustrated: 1 – Auvergne, France (Varet, 1969), 2 – Lovozero, 3 – Khibina (Bussen and Sakharov, 1972), 4 – Uganda (Tyler and King, 1967), 5 – Morotu, Sakhalin (Yagi, 1953), 6 – South Qoroq, South Greenland (Stephenson, 1972), 7 – Ilimaussaq (Larsen, 1976).

cations calculated to 6 oxygens. The general clinopyroxene formula is XYZ_2O_6 and, in alkaline environments, the tetrahedral site (*Z*) is occupied by Si, Al and Fe^{3+}. The *X* site is occupied mostly by Na and Ca, and *Y* is filled by the largest number of elements including Fe^{2+}, Mg, Mn, Ti, Zr and Al.

The analyses plotted in Figs 4 and 5 below are a sub-set totalling 110 analyses that have been selected from the full data-set of all 988 pyroxene analyses. One microprobe analysis from each height was selected for the sub-set with the main criterion for selection being that with the highest MgO content. This approach was undertaken in order to depict, as closely as possible, the most primitive (and therefore closest to cumulus) composition. It is likely that sub-solidus reactions had occurred for some samples, and that this has modified the original composition. However, it was not possible to establish whether, if any, sub-solidus modifications occurred solely from textural, or morphological features. Thus, whilst the analyses selected are from 'core' regions within individual pyroxene grains, we are not able to verify that each of the analyses selected represents the primary cumulus composition for that height. Nevertheless, we believe that this approach, when considered in terms of the complete stratigraphical section of 2.4 km, represents the best available attempt to interpret the Lovozero intrusion from the chemical analyses of the pyroxenes. (See also discussion below on cryptic variation.)

The present work, and that of earlier studies (Gerasimovsky *et al*., 1966; Korobeynikov and Laaioki, 1994) have demonstrated that Lovozero pyroxenes are members of the diopside–hedenbergite–aegirine series. For estimating the compositional evolution of the Lovozero pyroxenes we have used the parameter (Na-Mg), based on atomic proportions, as a fractionation index, plotted against elements expressed in formula units, as proposed by Stephenson (1972). The pyroxene trends illustrated in Figs 3 and 4, are characterized by strong Na and Fe^{3+} enrichments towards the aegirine apex, with hedenbergite (Ca,Fe) remaining approximately constant or decreasing slightly, but diopside (Ca,Mg) continuously decreasing. This trend is coupled with an increase in Ti except in some samples of very aegirine-rich pyroxenes, in which Ti decreases (Fig. 4). There is little variation in Al and Mn.

From these diagrams (Figs 3, 4) it is apparent that the major substitution during the evolution of the Lovozero clinopyroxenes is (Na,Fe^3,Ti) for (Ca,Mg,Fe^2). This statement is also supported by strong positive correlations of Na-Fe^{3+}, Mg-Ca, Fe^{3+}+2Ti-Na and negative correlations of Ca-Na with stoichiometric line slopes (not shown here). The scatter of points however, suggests that the substitution is probably more complex. Ti is probably present not only as $NaTiSiAlO_6$, but also partly as the neptunite component $Na_2FeTiSi_4O_{12}$ (Ferguson, 1977). The decrease of Ti in some of the highly evolved pyroxenes (Figs 4, 5) is probably connected with the complete absence of Fe^{2+} that is necessary for the formation of the neptunite component. Additionally, Ti may have been removed by incorporation into late-stage accessory Ti-minerals such as the lomonosovite-murmanite group or late lamprophyllite. Zr is an important component of the Lovozero clinopyroxenes. According to our data, and that from the literature (Njonfang and Moreau, 2000), the concentration of ZrO_2 can reach 2% in pyroxenes but drops with increasing pyroxene alkalinity. Jones and Peckett (1981) proposed that Zr is present as the component $Na(Fe^{2+},Mg)_{0.5}Zr_{0.5}Si_2O_6$. It is most probable that the component $NaZrSiAlO_6$ exists in the Lovozero

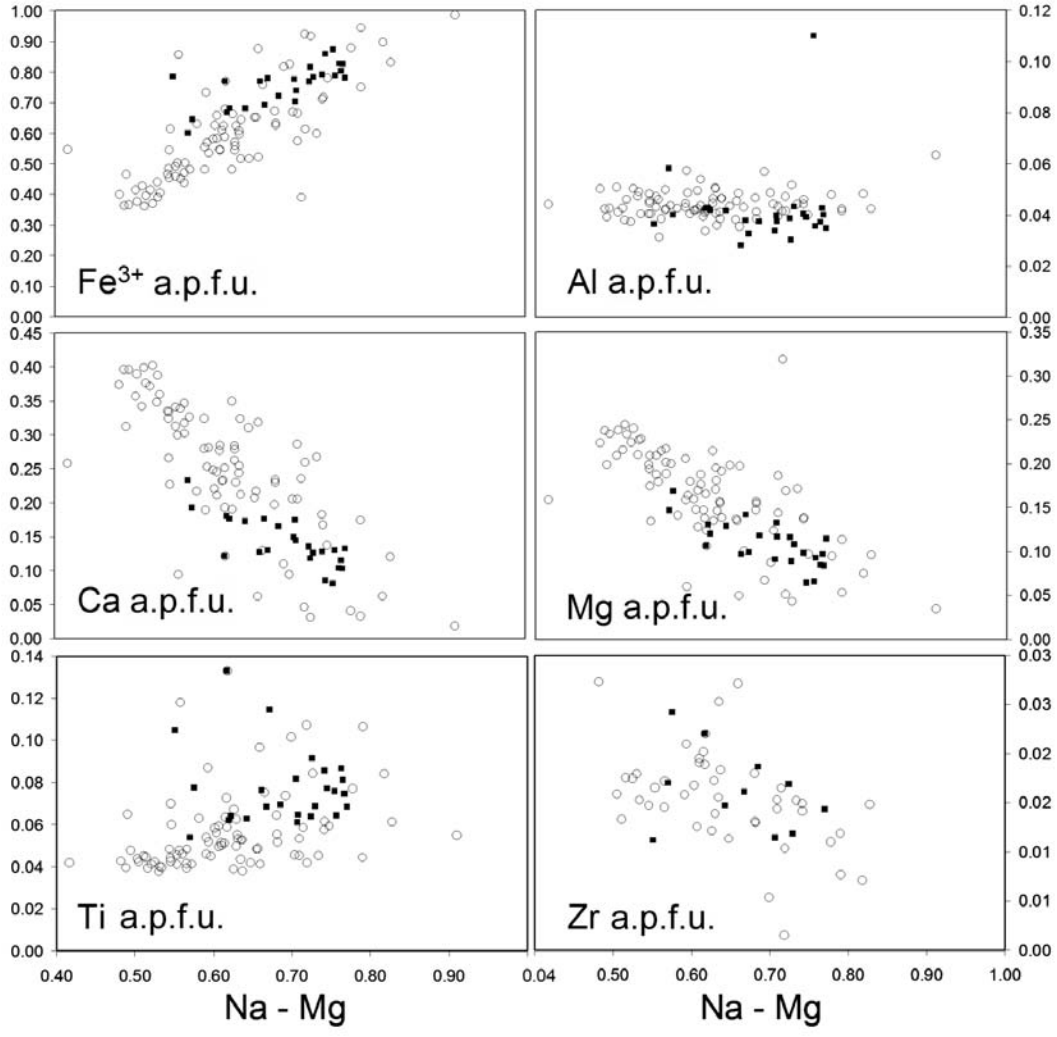

FIG. 4. Compositional variation in pyroxenes (representative analyses) in relation to the Na-Mg fractionation index (Na-Mg), expressed as cation proportions to 6 oxygens. Open circle = pyroxene from Differentiated Complex; filled square = pyroxene from Eudialyte Complex.

pyroxenes, as was proposed by Larsen (1976) for Ilimaussaq pyroxenes. At Lovozero, the pyroxene most enriched in Zr (up to 1.35% ZrO_2) occurs in the Differentiated Complex. Some pyroxenes from strongly evolved porphyritic eudialyte lujavrites contain up to 1.1% ZnO, where Zn probably substitutes for Fe^{2+} in the structure.

The compositional zoning in the Lovozero clinopyroxenes is very complex and generally the aegirine component increases in the crystal rims (Table 3), or in interstitial grains. It is interesting to note that the Zr content drops sharply in the pyroxene rims (Table 3). This could result from a decrease in Zr solubility in the pyroxenes with the rise of alkalinity (Njonfang and Moreau, 2000), or as a result of interstitial eudialyte crystallization, eudialyte being a major sink for Zr in the Lovozero rocks.

Cryptic layering

The most striking feature of pyroxene evolution at Lovozero is the regular change in cumulus pyroxene composition throughout the complete

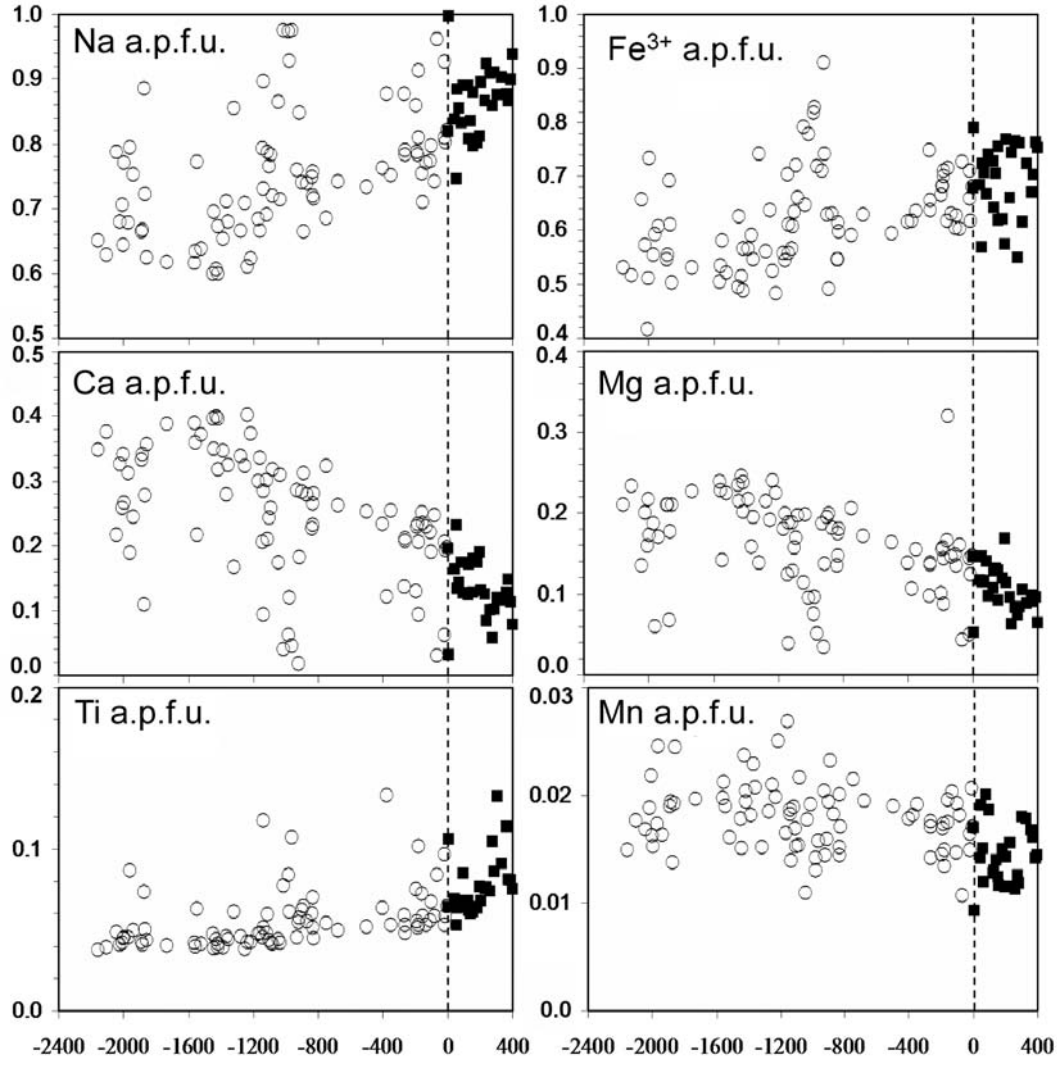

FIG. 5. Compositional variation in pyroxenes (as a.p.f.u.) plotted *vs*. height in the Lovozero intrusion. Zero (0) represents the contact between the Eudialyte and the Differentiated complexes. Negative values are the distances of the Differentiated Complex rocks from the contact; positive values are the depth of the Eudialyte Complex rocks from the contact. Open symbol = pyroxene from Differentiated Complex; filled symbol = pyroxene from Eudialyte Complex.

stratigraphic section of the pluton. Variations in pyroxene composition record subtle changes in alkaline magma composition very effectively. Such an approach is traditional and was applied successfully for the estimation of basic and ultrabasic magmatic evolution in layered intrusions (Eales and Cawthorn, 1996; Wilson *et al*., 1996). The detailed investigation of clinopyroxene chemical evolution in the stratigraphic section of a peralkaline intrusion is described for the first time in this paper. In order to minimize the influence of overprinting processes and to assess the evolution of pyroxene in the Lovozero massif we analysed only cores of well shaped (i.e. not interstitial) clinopyroxene grains, these being most likely to be cumulus in origin.

TABLE 3. Representative analyses (wt.%) of zoned pyroxene crystals from the upper part of the Differentiated Complex (sample no. Lovo 9, Fig. 1).

	SiO_2	TiO_2	Al_2O_3	Fe_2O_3	MnO	MgO	CaO	Na_2O	NiO	Cr_2O_3	ZrO_2	Total
core	51.4	2.15	0.98	23.5	0.58	3.59	7.71	9.26	n.d.	b.d.l.	0.91	100.0
rim	52.7	4.39	1.06	24.5	0.73	1.82	2.40	12.4	n.d.	0.01	0.01	100.1
core	51.8	1.63	0.89	24.3	0.52	3.22	7.18	9.73	n.d.	b.d.l.	0.87	100.1
rim	52.4	3.54	1.05	25.4	0.58	1.65	2.51	12.3	n.d.	0.03	0.04	99.5
							cations to 6 oxygens					
	Si	Ti	Al	Fe^{3+}	Mn	Mg	Ca	Na	Ni	Cr	Zr	Sum
core	1.95	0.06	0.04	0.67	0.02	0.20	0.31	0.68	0.00	0.00	0.02	3.96
rim	1.98	0.12	0.05	0.69	0.02	0.10	0.10	0.90	0.00	0.00	0.00	3.97
core	1.96	0.05	0.04	0.69	0.02	0.18	0.29	0.72	0.00	0.00	0.02	3.97
rim	1.99	0.10	0.05	0.72	0.02	0.09	0.10	0.90	0.00	0.00	0.00	3.98

All Fe as Fe_2O_3
b.d.l. = below detection limit
n.d. = not determined

In Fig. 5, element concentrations expressed as atoms per formula unit (a.p.f.u.) are plotted against structural depth within the intrusion, with zero being taken as the upper contact of the Differentiated Complex. All depths in Phase 2 (Differentiated Complex) are expressed as negative values, and in Phase 3 (Eudialyte Complex) as positive values. The cryptic variation observed in the pyroxene appears to be very substantial. With increasing stratigraphic height, the concentrations of Na, Fe^{3+} and Ti increase, whereas Mg, Ca (and Mn) decrease. There is generally a continuous change in the composition of the cumulus pyroxene throughout the Differentiated Complex, which indicates both an absence of magma replenishment and that the magma chamber was not chemically zoned before the crystallization commenced. An analogous plot for the most primitive pyroxenes (with the highest Ca and Mg contents) displays similar trends of pyroxene evolution. Correlation of Na, Ca, Mg, Ti, Mn and Fe^{+3} (a.p.f.u.) for primitive pyroxenes and depths are significant at the 95% level. The calculations were performed according to the method of Afifi and Azen (1979). The deviations of the compositions of primitive pyroxenes are likely to be related to the overprinting and floatation of small crystals of pyroxene from deeper parts of the Lovozero magma chamber. For instance, primary pyroxene becomes slightly more primitive from ~2200 m to ~1200 m probably as a result of mixing with pyroxene crystals moving upwards. More evolved pyroxene at ~1000 m is probably the result of reaction with more residual melt. In the case of the Eudialyte Complex, fluctuations of pyroxene composition may also be caused by reaction relationships of alkaline magma with the rocks of the roof of the intrusion, which are mainly alkaline basalts. These processes are developed most intensely in the central and eastern parts of the massif, but on the whole they are subordinate. The absence of a compositional gap between the pyroxenes of Phases 2 and 3 indicates the very close relationship between these intrusions, and that the Lovozero pluton effectively acted as a quasi-closed chemical system. The closed nature of the Lovozero magma fractionation is in accordance with the isotopic data (Kramm and Kogarko, 1994), and the character of the pyroxene cryptic layering suggests that fractional crystallization *in situ* of a single batch of peralkaline magma was the main process governing the formation of the layered Lovozero pluton.

Elsewhere, Kogarko and Khapaev (1987) and Kogarko *et al*. (2002) have proposed possible mechanisms for rhythmic layering in the Differentiated Complex. As outlined above, the Differentiated Complex is composed of layered units that (from base to top of each unit) comprise urtite, foyaite and lujavrite. Pyroxene is concentrated in the lujavrite layers, mainly occurring only as an interstitial phase in the urtites and foyaites. Several mechanisms have been proposed to explain this distribution (summarized by Kogarko *et al*., 2002). Kogarko and Khapaev

(1987) considered that pulses of convection combined with the varying hydraulic properties of different minerals could lead to layering, whereas for magmatic systems containing minerals with different settling velocities and different critical concentrations, Sparks *et al*. (1993) proposed that sequences of layers could result from steady convection and steady cooling. Crystals may remain in suspension only until the settling velocity is small as compared with the velocity of convective currents. At Lovozero, the primary cumulus pyroxene crystals, although of high density, remained longer in suspension, as compared with nepheline and feldspar, probably because of their small size (some crystals are only a few microns across) and acicular form, and hence low settling velocity, and therefore only settled towards the end of each cycle at the lujavrite stage. Thus, the pyroxene composition evolved steadily in step with evolution of the liquid.

The average bulk composition of the Eudialyte Complex is close to lujavrite. There is no rhythmic layering in these rocks although layering is present as alternating leucocratic and melanocratic lujavrites. The modal proportion of pyroxene increases towards the top of the Eudialyte Complex, probably also resulting from the lower settling velocity of pyroxene as compared with nepheline and feldspar. As can be seen from Fig. 5, the pyroxenes from the Eudialyte Complex continued to evolve in a similar manner (i.e. against height in the intrusion) to the Differentiated Complex. Cryptic variation of clinopyroxene is evident throughout the stratigraphic section of Lovozero and consistent with its formation by upward directed fractional crystallization in a quasi-closed system. However, it should be pointed out that reaction of alkaline magma with surrounding rocks complicated this process and the uppermost part of the intrusion has been removed during erosion and glaciation.

The range of compositional variation in pyroxene from different levels of the Differentiated Complex can be large, and the patterns of these trends are highly variable. Examples of this variability are illustrated in three examples from different stratigraphical horizons (Fig. 6).

The migration of interstitial melt through the pores of the partly consolidated rocks, as a result of compaction and convection within the settled crystals, is an important process in layered intrusions (Naslund and McBirney, 1996). The compositions of interstitial melts capable of migration throughout many hundreds of metres (Wilson *et al*., 1996) were not uniform and depend on many factors including chemistry of the crystalline mass in which the interstitial melts circulate, rate of percolation, extent of attainment of equilibrium between crystals and melt. After the formation of a continuous crystalline network, and when percolation ceases, the composition of a stagnant porous melt is mainly governed by the diffusion rates of components and by the compositions of minerals in close contact with the pyroxene growing within a confined space. Nevertheless, where sufficient data are available from individual layers of the Differentiated Complex (Fig. 6), one may conclude that the evolution of the interstitial melt, of which the composition varies considerably, was controlled by fractional crystallization, and it evolved in the same direction as for the intrusion as a whole. The resulting trend is dominated by the growth in alkalinity and decrease in Mg content. However, the combined evolution of the full suite of Lovozero pyroxenes is similar to that of other alkaline complexes (Figs 3, 4), and records the entire evolution of the undersaturated peralkaline magma systems from the liquidus to the final stages of crystallization.

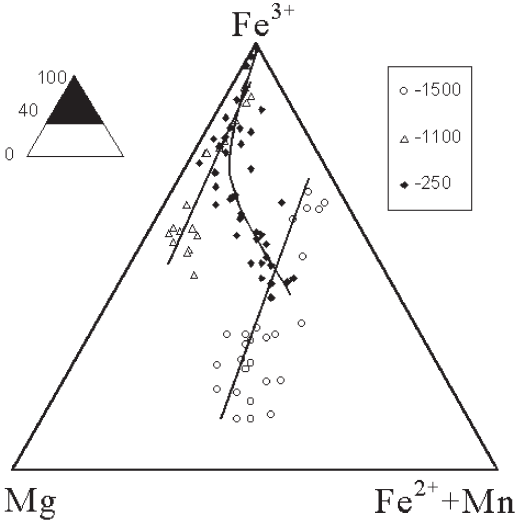

FIG. 6. Examples of the variability in compositional trends within pyroxenes at different heights within the Differentiated Complex, with the following symbols: open circle = –1500 m; open triangle = –1100 m; filled diamond = – 250 m.

Physical and chemical conditions of crystallization

From the experimental data on phase equilibria of Lovozero foyaitic and lujavritic compositions, it has been proposed (Kogarko, 1977) that the peralkaline magma of this complex crystallized over a wide temperature interval, the liquidus to solidus interval being >300ºC. Similar conclusions were drawn from melt equilibrium experiments on Illimaussaq rocks (Sood and Edgar, 1970). According to Mitchell and Platt (1978) the crystallization interval of the Coldwell alkaline complex ranges from 800–900 to 500–550ºC. Liquidus temperatures of the peralkaline syenites of the Mlanje massif, Malawi, were estimated at 800–900ºC by Platt and Woolley (1986). The Lovozero massif is considered, from geological data, to be a subvolcanic body (Bussen and Sakharov, 1972) and the maximum total pressure should not exceed 1.5 kbar (Kogarko, 1977). The agpaitic magma of the Lovozero massif is considered to be surprisingly dry (P_{H_2O} = 100–300 bar), which corresponds to ~0.7 wt.% H_2O (Kogarko *et al.*, 1977). It is inferred from the *P-T* melting curve of the average composition of Lovozero that in the initial stage of crystallization the water-vapour pressure was relatively low, resulting in the earlier, or at least simultaneous, crystallization of leucocratic minerals (nepheline + K-feldspar) and pyroxene. At higher water pressures alkaline pyroxene becomes the liquidus phase much earlier (100–150ºC higher than nepheline + K-feldspar). From these experiments the temperature interval of pyroxene separation was estimated at 970–700ºC.

The temperatures established for the Lovozero rocks from the melting experiments have been confirmed by an investigation of micro-inclusions in the minerals (Kogarko, 1977), the primary inclusions being the result of crystallization of trapped melts homogenized at temperatures in the range 1010–730ºC. High temperatures (1010–980ºC) of micro-inclusion homogenization in the earliest mineral phase (nepheline) also correspond on a P_{H_2O}-*T* diagram (Kogarko, 1987) to low water-vapour pressures of 100–200 bar. The accumulation of volatile components in residual melts, but not in the fluid phase because of high alkalinity (Kogarko, 1977), probably increased the interval of pyroxene crystallization from 970 to 450ºC (Kogarko, 1987).

The redox conditions of the Lovozero agpaitic magma have been estimated experimentally (Kogarko, 1987). The melanocratic mineral suite, including pyroxene and aenigmatite, was stable only under conditions close to the QFM buffer system. At higher oxygen fugacities (nickel-nickel oxide) aenigmatite becomes unstable and produces ilmenite and aegirine (Kogarko, 1987), while at lower f_{O_2} aegirine is substituted by Di- and Hd-rich pyroxene. Accurate thermodynamic calculations of the reaction are not possible at present because the free-energy data for solid solutions of aenigmatite, aegirine and mangano-ilmenite are not available. According to semi-quantitative calculations, the stability field of the mineral association aegirine-aenigmatite-ilmenite in peralkaline environments occurs in the magmatic temperature range 1000–600ºC, and in a f_{O_2} regime higher than the nickel-nickel-oxide buffer (Carmichael and Nicholls, 1967). This discrepancy with our experimental data may be explained by the considerable errors (uncertainties) arising from the estimation of the free energy of ilmenite and aenigmatite as pure solid-solution end-members, since in Lovozero the composition of these mineral phases are much more complex.

In all the Lovozero rocks, aegirine is very closely associated with arfvedsonite that commonly contains more then twice as much ferrous as ferric iron (Gerasimovsky *et al*., 1966). According to the experimental data of Ernst (1962), the stability field of arfvedsonite with a similar Si/(Na+Fe+Si) ratio to that of the Lovozero amphibole occurs, even under lower f_{O_2}, between the iron-wüstite and QFM buffer systems. Ernst (1962) also found that the stability temperatures of arfvedsonite increased substantially with a decrease in oxygen fugacity. The very large field of alkaline amphibole crystallization in Lovozero rocks suggests that the oxygen fugacity in these rocks was very close to the QFM buffer system (~10^{-14} to -10^{-20} bar in the temperature range 900–650ºC).

It is widely accepted that in magmatic systems the ferric-ferrous equilibrium is controlled by oxygen fugacity, temperature and melt composition. In the light of acid-base interaction theory (Korzhinsky, 1959), increasing melt alkalinity results in a decrease in the activity of the less basic components and production of more oxidized forms of elements, such as ferric Fe at the expense of ferrous. In the following reaction the increase of melt alkalinity results in decreasing $X_{FeO_{1.5}}/Y_{FeO}$ ratio and is accompanied by an increase in the Fe^{3+}/Fe^{2+} ratio under constant f_{O_2}.

$$4FeO_{melt} + O_2 = 4FeO_{1.5\ melt}$$
$$K = M^4FeO_{1.5}X^4_{FeO_{1.5}}/N^4_{FeO}Y_{FeO}f_{O_2}$$

(where X and Y are the activity coefficients, and M and N are mole fractions).

We assume that the alkalinity enrichment during the progressive differentiation of the Lovozero magma provided the major chemical control for the evolution of the pyroxenes.

As was shown by Gerasimovsky *et al*. (1966) and Kogarko *et al*. (2002), the pyroxene and associated Fe-Mn-Ti-bearing accessory minerals mutually change chemically through all phases of the Lovozero intrusion, including the stratigraphic section of the Differentiated Complex. In Phase 1 and the lowermost zone (2300−1600 m) the pyroxene is associated with a miaskitic mineral assemblage of euhedral magnetite, with exsolved Mn ilmenite, amphibole, mosandrite, Fe sulphides and titanite. In the upper zone of Phase 2 (1600−~600 m), magnetite disappears and an assemblage of Mn-ilmenite, pyroxene and aenigmatite is usual. In the uppermost section of the Differentiated Complex, Mn-ilmenite is generally substituted by lorenzenite. The reaction Mn-ilmenite + liquid = lorenzenite was also found in interstitial environments in the lowermost part of Phase 2, suggesting an extremely rapid increase in alkalinity in the trapped melt. In the Eudialyte Complex (Phase 3) the most evolved pyroxenes (dramatically enriched in aegirine component) are associated with a more alkaline suite of Fe-Mn-Ti minerals than in Phases 1 and 2, and include lamprophyllite, murmanite and lorenzenite, which all became cumulus phases in Phase 3 (Kogarko *et al.*, 2002). Aenigmatite is not present in the Eudialyte Complex, perhaps because of the following reaction that occurs in more alkaline and evolved environments:

$$\underset{\text{aenigmatite}}{2Na_2Fe_5TiSi_6O_{20}} + \underset{\text{melt}}{12SiO_2} + 4Na_2O + 2O_2 = \underset{\text{aegirine}}{10NaFeSi_2O_6} + \underset{\text{lorenzenite}}{Na_2Ti_2Si_4O_{12}}$$

Thus, the pyroxene crystallization in the Lovozero intrusion was characterized by reducing conditions (approximating to the QFM buffer).

Summarizing the published data one may conclude that alkaline rocks can form under extremely variable redox conditions. Alkaline basalts from Trindade Island (Brazil), including late peralkaline differentiates (Ryabchikov and Kogarko, 1994), show relatively high oxygen fugacities. Extremely high oxygen fugacities (1 to 2 log units above QFM buffer) were found for high-Mg effusives and dyke rocks (meimechites and alkali picrites) from the Russian Maimecha-Kotuy province of alkaline and peralkaline rocks and carbonatites (Ryabchikov *et al*., 2002; Sobolev *et al*., 1991). Even higher oxygen fugacities were estimated for the Gronnedal-Ika carbonatite-syenite complex, South Greenland (Halama *et al*., 2005).

Low oxygen fugacities, possibly reaching the field of Fe-Ni alloy stability, were reported for the peralkaline Ilimaussaq massif in South Greenland (Markl *et al*., 2001; Marks and Markl, 2001). It has also been suggested that f_{O_2} increased during the evolution of the Ilimaussaq magmatic system, during the late stages exceeding the QFM buffer (Markl *et al*., 2001; Marks and Markl, 2001). As has been deduced from the Fe-Ti oxides + titanite + clinopyroxene mineral assemblage, the apatite-bearing intrusion of the Khibina alkaline complex is characterized by oxygen fugacities close to the QFM buffer (Ryabchikov and Kogarko, 2006), and in this respect, this magmatic system is similar to the neighbouring Lovozero complex.

Acknowledgements

This work was partly supported by RFBR Grants N 02-05-74006 and 00-15-98497, a Royal Society Grant for fieldwork for CTW and ARW, and a visit of LK to London (NATO Grant EST.CLG 975118). We would like to thank three anonymous referees for their constructive comments.

References

Afifi, A.A. and Azen, S.P. (1979) *Statistical Analysis: A Computer Oriented Approach*, 2nd edition. Academic Press, New York, 488 pp.

Arzamastsev, A.A., Arzamastseva, L.V., Glasnev, V.N. and Raevsky, A.B (1998) Deep structure and the composition of deep parts of Khibina and Lovozero complexes, Kola Peninsula, petrological and geophysical model. *Petrologiya*, **46**, 478−496 (in Russian).

Bussen, I.V. and Sakharov, A.S. (1972) *Petrology of the Lovozero Alkaline Massif* (in Russian). Nauka, Leningrad, 296 pp.

Carmichael, I.S.E. and Nicholls, J. (1967) Iron-titanium oxides and oxygen fugacities in volcanic rocks. *Journal of Geophysical Research*, **72,** 4665−4687.

Clark, A.M. (1993) *Hey's Mineral Index. Mineral Species, Varieties and Synonyms.* Chapman & Hall,

London, 852 pp.

Eales, H.V. and Cawthorn, R.G. (1996) The Bushveld Complex. Pp. 181–229 in: *Layered Intrusions* (R.G. Cawthorn, editor). Developments in Petrology, **15**. Elsevier, Amsterdam.

Ernst, W.G. (1962) Synthesis, stability relations and occurrence of riebeckite and riebeckite-arfvedsonite solid solutions. *Journal of Geology*, **70,** 689–736.

Ferguson, A.K. (1977) The natural occurrence of aegirine-neptunite solid solution. *Contributions to Mineralogy and Petrology*, **60,** 247–253.

Gerasimovsky, V.I., Volkov, V.P., Kogarko, L.N., Polyakov, A.I., Saprykina, T.V. and Balashov, Yu.A. (1966) *The Geochemistry of the Lovozero Alkaline Massif. Part 1. Geology and Petrology. Part 2. Geochemistry.* Translated 1968 by D.A. Brown. Australian National University Press, Canberra, pp. 224 and 369 pp. (translation of original Russian text published in 1966).

Halama, R., Vennemann, T., Siebel, W. and Markl, G. (2005) The Gronnedal-Ika carbonatite-syenite complex, South Greenland: carbonatite formation by liquid immiscibility. *Journal of Petrology*, **46**, 191–217.

Jones, A.P. (1984) Mafic silicates from the nepheline syenites of the Motzfeldt centre, South Greenland. *Mineralogical Magazine*, **48,** 1–12.

Jones, A.P. and Peckett, A. (1981) Zirconium-bearing aegirines from Motzfeldt, south Greenland. *Contributions to Mineralogy and Petrology*, **75,** 251–255.

Kogarko, L.N. (1977) *Genetic Problems of Agpaitic Magmas.* Nauka, Moscow, 294 pp. (in Russian).

Kogarko, L.N. (1987) Alkaline rocks of the eastern part of the Baltic Shield (Kola Peninsula). Pp. 531–544 in: *Alkaline Igneous Rocks* (J.G. Fitton and B.G.J. Upton, editors). Special Publication **30,** Geological Society, London.

Kogarko, L.N. and Khapaev, V. (1987) The modelling of formation of apatite deposits of the Khibina massif (Kola Peninsula). Pp. 589–611 in: *Origin of Igneous Layering* (I. Parsons, editor). Reidel Publishing Company, Dordrecht, The Netherlands.

Kogarko, L.N., Burnham, C.W. and Shettle, D. (1977) The water regime in hyperalkaline magmas (in Russian). *Geokhimiya*, **5**, 643–651.

Kogarko, L.N., Kononova, V.A., Orlova, M.P. and Woolley, A.R. (1995) *Alkaline Rocks and Carbonatites of the World. Part 2. Former USSR.* Chapman & Hall, London, 226 pp.

Kogarko, L.N., Williams, C.T. and Woolley, A.R. (2002) Chemical evolution and petrogenetic implications of loparite in the layered, peralkaline Lovozero complex, Kola peninsula, Russia. *Mineralogy and Petrology*, **74,** 1–24.

Korobeynikov, A.N. and Laaioki, K. (1994) Petrological aspects of the evolution of clinopyroxene composition in the intrusive rocks of the Lovozero alkaline massif. *Geochemistry International*, **31,** 69–76.

Korzhinsky, D.S. (1959) Acid-basic interaction of the components in silicate melts and the direction of the cotectic lines. *Doklady of the Academy of Sciences of the USSR. Earth Science Sections*, **128,** 821– 823.

Kramm, U. and Kogarko, L.N. (1994) Nd and Sr isotope signatures of the Khibina and Lovozero agpaitic centres, Kola alkaline province, Russia. *Lithos*, **32,** 225–242.

Larsen, L.M. (1976) Clinopyroxenes and coexisting mafic minerals from the alkaline Ilimaussaq intrusion, South Greenland. *Journal of Petrology*, **17,** 258–290.

Mandarino, J.A. (1999) *Fleischer's Glossary of Mineral Species* (8th edition). Mineralogical Record, Tucson, Arizona, USA, 225 pp.

Markl, G., Marks, M., Schwinn, G. and Sommer, H. (2001) Phase equilibrium constraints on intensive crystallization parameters of the Ilimaussaq Complex, South Greenland. *Journal of Petrology*, **42**, 2231–2258.

Marks, M. and Markl, G. (2001) Fractionation and assimilation processes in the alkaline augite syenite unit of the Ilimaussaq Intrusion, South Greenland, as deduced from phase equilibria. *Journal of Petrology*, **42**, 1947–1969.

Mitchell, R.H. and Platt, R.G. (1978) Mafic mineralogy of ferroaugite syenite from the Coldwell alkaline complex, Ontario, Canada. *Journal of Petrology*, **19,** 627–651.

Naslund, H.R. and McBirney, A.R. (1996) Mechanisms of formation of igneous layering. Pp. 1-43 in: *Layered Intrusions* (R.G. Cawthorn, editor). Developments in Petrology, **15**. Elsevier, Amsterdam.

Njonfang, E. and Moreau, C. (2000) The mafic mineralogy of the Pande Massif, Tikar Plain, Cameroon. *Mineralogical Magazine*, **64,** 525–537.

Platt, R.G. and Woolley, A.R. (1986) The mafic mineralogy of the peralkaline syenites and granites of the Mulanje complex, Malawi. *Mineralogical Magazine*, **50,** 85–99.

Ryabchikov, I.D. and Kogarko, L.N. (1994) Redox equilibria in alkaline lavas from Trindade Island, Brasil. *International Geology Review*, **36**, 173–183.

Ryabchikov, D. and Kogarko, L.N. (2006) Magnetite compositions and oxygen fugacities of the Khibina magmatic system. *Lithos*, in press.

Ryabchikov, I.D., Solovova, I.P., Kogarko, L.N., Bray, G.P., Ntaflos, Th. and Simakin, S.G. (2002) Evidence for melt inclusions. *Geochemistry International*, **40**, 1031–1041.

Sobolev, A.V., Kamenetskaya, V.S. and Kononkova, N.N., (1991) New data on petrology of Siberian

meimechites. *Geochemistry International*, **8**, 1084–1095.

Sood, M.K. and Edgar, A.B. (1970) Melting relations of undersaturated alkaline rocks from the Illimaussaq intrusion and Gronnedal-Ika complex South Greenland, under water vapour and controlled partial oxygen pressure. *Meddelelser om Grønland*, **181(12)**, 1–41.

Sparks, R.S.J., Huppert, H.E., Koyaguchi, T. and Hallworth, M.A. (1993) Origin of modal and rhythmic igneous layering by sedimentation in a convecting magma chamber. *Nature, London*, **361,** 246–249.

Stephenson, D. (1972) Alkali clinopyroxenes from nepheline syenites of the South Qoroq Centre, South Greenland. *Lithos*, **5,** 187–201.

Tyler, R.C. and King, B.C. (1967) The pyroxenes of the alkaline igneous complexes of Eastern Uganda. *Mineralogical Magazine*, **36,** 5–22.

Varet, J. (1969) Les pyroxenes des phonolites du Cantal (Auvergne, France). *Neues Jahrbuch für Mineralogie Monatshefte*, **4,** 174–84.

Vlasov, K.A., Kuz'menko, M.Z. and Es'kova, E.M. (1966) *The Lovozero Alkali Massif*. Oliver and Boyd, Edinburgh, 627 pp. (first published in 1959 by Akademii Nauk SSSR, Moscow).

Wilson, J.R. and Sorensen, H.S. (1996) The Fongen-Hyllingen layered instrusive complex, Norway. Pp. 303–329 in: *Layered Intrusions* (R.G. Cawthorn, editor). Developments in Petrology, **15**. Elsevier, Amsterdam.

Yagi, K. (1953) Petrochemical studies of the alkalic rocks of the Morotu district, Sakhalin. *Geological Society of America Bulletin*, **64,** 769–810.

[*Manuscript received 8 August 2005: revised 15 September 2006*]